coatings

MDPI

Article

Oxygen Barrier Performance of Poly (Vinyl Alcohol) Coating Films with Different Induced Crystallinity and Model Predictions

Alamin Idris [1,*], Adrian Muntean [2], Beko Mesic [1,*], Magnus Lestelius [1] and Asif Javed [1]

[1] Department of Engineering and Chemical Sciences, Karlstad University, SE 651 88 Karlstad, Sweden; magnus.lestelius@kau.se (M.L.); asif.javed@kau.se (A.J.)
[2] Department of Mathematics and Computer Sciences, Karlstad University, SE 651 88 Karlstad, Sweden; adrian.muntean@kau.se
* Correspondence: alamin.abdulgadir@kau.se (A.I.); behudin.mesic@kau.se (B.M.)

Abstract: The presence of the crystalline regions in poly (vinyl alcohol) coating films acts as barrier clusters forcing the gas molecules to diffuse in a longer pathway in the amorphous region of the polymer, where diffusivity and solubility are promoted in comparison. Evaluating the influence of crystalline regions on the oxygen barrier property of a semi-crystalline polymer is thus essential to prepare better coating films. Poly (vinyl alcohol) coating films with varying induced crystallinity were prepared on a polyethylene terephthalate (PET) substrate by drying at different annealing temperatures for 10 min. The coating films were first delaminated from the PET substrate and then characterized using Fourier transform infrared (FTIR) spectroscopy, differential scanning calorimetry (DSC), and X-ray diffraction (XRD) techniques to determine and confirm the induced percentage of crystallinity. The barrier performance of the coating films, i.e., the oxygen transmission rate (OTR), was measured at room temperature. Results showed a decrease in the OTR values of poly (vinyl alcohol) film with an increase in the degree of crystallinity of the polymer matrix. Tortuosity-based models, i.e., modified Nielsen models, were adopted to predict the barrier property of the semi-crystalline PVOH film with uniform or randomly distributed crystallites. A modified Nielsen model for orderly distributed crystallites with an aspect ratio of 3.4 and for randomly distributed crystallites with an aspect ratio of 10.4 resulted in a good correlation with the experimental observation. For the randomly distributed crystallites, lower absolute average relative errors of 4.66, 4.45, and 5.79% were observed as compared to orderly distributed crystallites when the degree of crystallinity was obtained using FTIR, DSC, and XRD data, respectively.

Keywords: barrier property; crystallinity; coating film; model predictions; poly (vinyl alcohol)

Citation: Idris, A.; Muntean, A.; Mesic, B.; Lestelius, M.; Javed, A. Oxygen Barrier Performance of Poly (Vinyl Alcohol) Coating Films with Different Induced Crystallinity and Model Predictions. *Coatings* **2021**, *11*, 1253. https://doi.org/10.3390/coatings11101253

Academic Editor: Stefano Farris

Received: 21 September 2021
Accepted: 12 October 2021
Published: 15 October 2021

1. Introduction

Poly (vinyl alcohol) (PVOH, [-CH_2-CHOH-]$_n$) is the largest volume of synthetic polymer produced worldwide. It is a water-soluble, linear, and non-halogenated aliphatic polyhydroxy polymer. PVOH is a semi-crystalline polymer well-known for its low oxygen permeability, good thermal resistance, excellent adhesive properties, and resistance to organic solvents, in addition to its attractive biocompatibility and biodegradability properties [1,2]. These desirable properties of PVOH have resulted in a wide range of practical applications, mainly in food packaging, biomedical materials, ultrafiltration membranes, ion exchange membranes, gas separation membranes, protective/binding coatings, etc. [3]. In addition, PVOH's low oxygen permeability, adhesive qualities, and effectiveness in film-forming are attractive properties for dispersion barrier coating applications. Moreover, PVOH is a recyclable, odour barrier, and food contact compliant, appropriate for active and antibacterial packaging [4,5], dry, and bulk food packaging applications [6,7]. The gas barrier property of PVOH is partially attributed to the crystalline regions/phases within its

matrix. These crystalline regions are comprised of the platy-like lamellae (single crystals) with the thickness of 10 to 20 nm bound to each other by disordered chains [8].

The degree of crystallinity of PVOH depends on the synthetic process conditions and physical aging [3]. The degree of crystallinity is thus a crucial structural characteristic that determines the macroscopic properties of the material. Improved mechanical strength, water resistance, and gas barrier properties can be obtained if the degree of crystallinity is increased. Hence, the determination of crystalline phase contents/degree of crystallinity from quantitative data is important to elucidate, predict, and optimize the properties of the PVOH polymer. There are various techniques commonly employed for the quantification of the degree of crystallinity in polymer systems. Among these measurement techniques, Fourier transform infrared (FTIR) spectroscopy [9,10], differential scanning calorimetry (DSC) [11,12], X-ray diffraction (XRD), nuclear magnetic resonance (NMR) spectroscopy [13], and density measurement [14] are commonly used. The IR technique provides a highly sensitive and indirect method to determine the degree of crystallinity of polymers, whereas X-ray diffraction provides a direct and efficient method, but requires costly equipment and a longer analysis time. For the case of the density measurement method, determination of crystallinity requires densities of complete amorphous and crystalline phases. This method cannot be used for semi-crystalline polymers, as 100% amorphous or 100% crystalline PVOH samples are unknown. The calorimetric measurement provides information on crystallinity for PVOH samples near its melting point. The degree of crystallinity is obtained from the conditions observed during the heating events on the sample. NMR spectroscopy can also be utilized to evaluate the degree of crystallinity based on the proton contents with restricted mobility [13]. However, the restriction of proton mobility may also arise from the formation of disordered aggregates with strong intermolecular interactions. Therefore, for reliable results, the technique requires the source of proton mobility restrictions to be distinguished. Other techniques, such as atomic pair distribution function [15], Raman spectroscopy [16,17], etc., were also used to quantify and analyse the crystal structures in polymeric materials.

The crystalline regions of the polymer system have lower gas solubility [18,19], and hence, they affect oxygen permeability through the polymer film. It is considered that crystalline regions act as a barrier to gas transport, restricting the diffusing gas molecules to follow a tortuous path. Therefore, it is convenient to adopt a tortuosity-based model to describe the influence of crystalline regions on the gas barrier property. Picard et al. [20] modified the Maxwell tortuosity model to predict the oxygen permeabilities in polylactide (PLA) film with varying crystallinity. Further, Duan and Thomas [21] used the Nielsen tortuosity model to predict water vapour permeability in Polylactic acid. According to their results, the model predictions showed a good agreement with experimental data. However, in both cases, the models' predictions were performed with the assumption of orderly distributed crystallites. In the current study, the Nielsen models for orderly and randomly distributed crystallites, are considered to predict oxygen permeability in PVOH coating films.

Therefore, this work aimed to prepare PVOH coating films with different induced crystallinity and model their effects on the oxygen barrier performances. To affect the percentage crystallinity of PVOH coating film, the annealing temperatures of the coated PVOH solution were varied for a predetermined time. The corresponding percentage crystallinities of the prepared PVOH films were then characterized using Fourier transform infrared (FTIR) spectroscopy, X-ray diffraction (XRD), and differential scanning calorimetry (DSC). The oxygen barrier performances of PVOH films with different crystallinity were measured using a Mocon Ox-Tran oxygen transmission rate tester at room temperature. The modified Nielson models accounting for the random and regular distribution of barrier inclusions were proposed to predict the barrier performance of PVOH coating films.

2. Materials and Methods

2.1. Materials

The polymer material, i.e., poly (vinyl alcohol) (PVOH) 6/98 grade, was supplied by Kuraray Europe Nordic AB OY, Vantaa, Finland The substrate film, i.e., polyethylene terephthalate (PET) with 297 mm width × 420 mm length × 0.118 mm thickness, was purchased from Robert Matton AB, Stockholm, Sweden. Deionized water was used as a solvent to dissolve PVOH granules.

2.2. Preparation of PVOH Coating Films

In a conical flask with a 500 mL capacity, 225 gm of deionized water was added to 25 gm of PVOH. The PVOH was cooked in a boiling water bath for 30 min under continuous mixing at 400 rpm with a dispersion blade impeller (IKA RW 20, Buck & Holm, Herlev, Denmark). The temperature of the PVOH solution was cooled from about 95 °C to room temperature under slow stirring with a magnetic stirrer to avoid bubble formations. The dissolved solid content was measured using an IR balance moisture analyzer (Model MA40, Sartorius Lab Instruments GmbH & Co KG, Goetingen Germany) to cross-check if any substantial amount of water was lost due to evaporation during the dissolution of PVOH. Further, the viscosity of the PVOH solution was measured using a Brookfield viscometer (Model RV-DVI+ Viscometer, Brookfield, Stoughton, MA, USA) to confirm the processability of the coating solution.

The PET films were first cut to 297 mm × 210 mm and used as a substrate material to prepare the PVOH coating films using a laboratory bench coater (K202 Control Coater, RK Coater Instruments Ltd., Royston, UK). The coating solution was applied to the PET substrate with a 6 m/min coater speed and coating rod of wire-wound diameter 1.27 mm, giving a nominal wet thickness of 100 µm. Then, the coated solution on the PET substrate was annealed in a drying oven for 10 min. An annealing time of 10 min was chosen to ensure the complete removal of the solvent, except for the first sample was annealed at 25 °C and left overnight to dry. The annealing temperatures and sampling names used are shown in Table 1. A total of four replicas of each PVOH film sample were fabricated on the PET substrate. The dried samples were stored in a controlled environment at 23 °C and 50% RH prior to their characterization and performance evaluation.

Table 1. Sample names and annealing conditions of PVOH coating films.

S. No.	Sample Name	Annealing Temperature (°C)	Annealing Time (min)
1	PVOH-RT	25	10
2	PVOH-60	60	10
3	PVOH-100	100	10
4	PVOH-120	120	10
5	PVOH-160	160	10

2.3. Characterization

The prepared PVOH coating films on the PET substrate were first delaminated physically, and their corresponding film thicknesses were measured to be 10 ± 2 µm (see Table S1). These samples were used to characterize the percentages of crystallinity induced, whereas the PVOH films with the PET substrate were used for oxygen barrier performance measurement.

2.3.1. Fourier Transform Infrared Spectroscopy

The delaminated thin PVOH films were characterized using the Fourier transform infrared (FTIR-ATR) Spectroscopy (Cary 30 FTIR, Agilent Technologies, Santa Clara, CA, USA). At least six trails were scanned at the wavelength range of 2000–1000 cm^{-1}. An av-

erage of six spectrums was considered for the calculation of the percentage crystallinity. The percentage crystallinity of PVOH coating films was obtained as follows:

$$\chi_c^{FTIR}(\%) = a + b\left(\frac{I_c}{I_a}\right), \quad (1)$$

where a and b are correlation coefficients. For PVOH polymer, the values of these coefficients are assigned as −13.1 and 89.5, respectively [22]. I_c and I_a are the IR absorbance intensities of peaks corresponding to the crystalline phase at a wavenumber range of 1140–1145 cm^{-1} and the amorphous phase at a wavenumber around 1090–1096 cm^{-1}, respectively [23].

2.3.2. Differential Scanning Calorimetry

The crystallinity of the PVOH polymer films was also measured using the differential scanning calorimetry (DSC, Q2000, TA Instrument, New Castle, DE, USA). About 6–8 mg of the delaminated PVOH films were scanned in heating mode used for the analysis. The DSC was first equilibrated at 0 °C and heated at a rate of 10 °C/min to 250 °C, with nitrogen gas purging maintained at 50 mL/min. The crystallinity of the polymer is calculated from heat of fusion/melting according to the expression [24]:

$$\chi_c^{DSC}(\%) = \frac{\Delta H_f}{\Delta H_f^o} \times 100, \quad (2)$$

where ΔH_f and ΔH_f^o are the enthalpy of fusion/melting of the PVOH film sample and PVOH polymer with 100% crystallinity in J/g, respectively. The melting enthalpy of PVOH at 100% crystallinity (ΔH_f^o) is 138.7 J/g [25,26].

2.3.3. X-ray Diffraction

The crystallinity of the delaminated PVOH coating films was also analyzed using the X-ray diffraction (XRD) technique (Empyrean, PANalytical, Malvern, UK). Samples were scanned within the scattering angle (2θ) ranging from 2° to 60° using the standard nickel filtered CuKα X-ray radiation source with a wavelength of 1.542 Å, operated at 35 kV and 25 mA. The percentage crystallinity of the PVOH coating film can be calculated from the area of the crystalline and amorphous peaks [27,28].

$$\chi_c^{XRD}(\%) = \frac{A_c}{A_c + A_a} \times 100, \quad (3)$$

where A_c and A_a are the area of the crystalline and amorphous phase peaks, respectively.

2.4. Barrier Performance Measurements

The oxygen barrier properties of the uncoated PET substrate and the PVOH coated films were measured for 5 cm^2 surface samples placed in an aluminium mask using a Mocon Ox-Tran oxygen transmission rate tester (Model 2/21 MH, Mocon, Minneapolis, MN, USA). The oxygen transmission rate (OTR) values were determined according to test method ASTM D 3985-05 [29], at 23.0 ± 1 °C, 50% relative humidity (RH), and 1 atm (760 mmHg) pressure difference across the sides of the sample. The concentration of permeant gas is 100%. The OTR measurements of each sample were performed for at least two replicates. The oxygen permeability coefficient is then calculated as [30]:

$$P_{O_2} = \frac{OTR}{\Delta p} \times t, \quad (4)$$

where P_{O_2} is the oxygen permeability coefficient in [mL·μm·m^{-2}·(24 h)$^{-1}$·atm^{-1}], Δp is the partial pressure difference of oxygen across the sides of the film (atm), and t is the combined thickness of the substrate and coating film.

2.5. Proposed Models

Crystalline phase fractions of polymer films appear to act as barrier domains to the permeant gas [31]. Hence, the decrease in oxygen gas permeability can be better described by the prolonged tortuous diffusion pathways. Nielsen models for orderly and randomly distributed barrier domains are proposed to predict the barrier property for the PVOH coating film with different percentage crystallinities. The model described the increased diffusion path length due to the obstacles formed by the barrier domains, such as particles or crystallites.

The generalized Nielsen model is given as [32]:

$$\frac{P}{P_o} = \frac{\phi_p}{\tau}, \tag{5}$$

where P and P_o are the oxygen permeability of the composite polymer film and pure polymer film in (mL·µm·m^{-2}·h^{-1}·atm^{-1}), respectively. Whereas φ_p is the volume fraction of the polymer phase and τ is the tortuosity factor defined as follows [33]:

$$\tau = \frac{Diffusion\ path\ length}{Film\ thickness}. \tag{6}$$

The maximum possible value for the tortuosity factor for evenly distributed barrier domains is provided by [32]:

$$\tau = 1 + (L/2W)\phi_d, \tag{7}$$

and similarly, the tortuosity factor for randomly distributed barrier domains can be expressed as [34]:

$$\tau = 1 + (1/3)(L/2W)\phi_d, \tag{8}$$

where φ_d is the volume fraction of inorganic fillers. The above model is developed for a composite film system composed of a polymer phase and inorganic phase. Analogically, a polymer system can be adopted, which comprises of an amorphous phase and crystalline phase. In this case, the crystallites are considered as barrier clusters responsible for the reduction in oxygen permeability.

For semi-crystalline polymers, the platy crystallites are assumed to be an impermeable domain with the aspect ratio $\alpha = L/W$. Therefore, the filler volume fraction in a composite system can be conveniently exchanged by the crystallinity fraction (χ_c) in the polymer matrix. Thus, for evenly distributed crystallites, the tortuosity factor is thus:

$$\tau = 1 + (\alpha/2)\chi_c. \tag{9}$$

And similarly, for randomly distributed crystallites across the polymer film, the tortuosity factor is:

$$\tau = 1 + (1/3)(\alpha/2)\chi_c. \tag{10}$$

Combining Equations (5) and (9) leads to the modified Nielsen model for orderly distributed crystallite domains.

$$\frac{P_{sc}}{P_{am}} = \frac{1 - \chi_c}{1 + (\alpha/2)\chi_c}, \tag{11}$$

where P_{sc} and P_{am} are the permeability coefficients of semi-crystalline polymer and amorphous phase in (mL·µm·m^{-2}·h^{-1}·atm^{-1}), respectively. Similarly, using Equations (5) and (10), the modified Nielsen model for randomly distributed crystallites can be expressed as follows:

$$\frac{P_{sc}}{P_{am}} = \frac{1 - \chi_c}{1 + (1/3)(\alpha/2)\chi_c}. \tag{12}$$

The precision of model predictions can be evaluated in terms of percentage average absolute relative errors (*AARE*%) as [35]:

$$AARE\% = \frac{100}{N}\sum_{1}^{N}\left|\frac{(P_{sc}/P_{am})_{pre} - (P_{sc}/P_{am})_{exp}}{(P_{sc}/P_{am})_{exp}}\right|, \quad (13)$$

where $(P_{sc}/P_{am})_{pre}$ and $(P_{sc}/P_{am})_{exp}$ are the predicted and experimental relative permeability. N is the number of data points.

3. Results and Discussion

3.1. Degree of Crystallinity of PVOH

The delaminated PVOH films were characterized using FTIR-ATR, and at least six random locations were scanned, with the average spectra presented in Figure 1. The crystallinity of PVOH coating films was determined from the ratio of intensities of absorption bands/peaks corresponding to the crystalline phase and amorphous phase. The absorbance band at 1143 cm^{-1} indicates the stretching vibration of C–O originating from the crystalline region of PVOH. The intensity of this band is related to the crystalline phase of the polymer chains [36]. It is associated with either stretching C–O of the chain with intermolecular H bonding of two hydroxyl groups on the same carbon chain plane, or the symmetric C–C stretching mode. The peak at 1093 cm^{-1} corresponds to the stretching vibration of C–O from the amorphous phase of the PVOH polymer [37]. Hence, the ratio of the intensities of the crystalline and amorphous peaks reflects the crystallinity of the PVOH. According to Equation (1), the percentage crystallinity calculated is presented in Table 2.

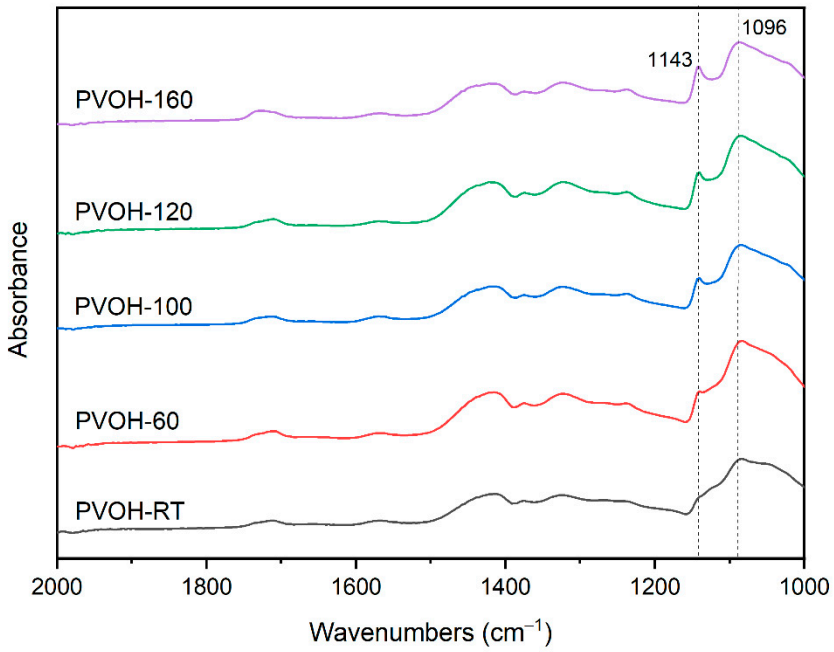

Figure 1. FTIR absorbance spectra for PVOH coating films prepared at different annealing temperatures.

Results showed that an increase in the degree of crystallinity was observed with the increased annealing temperatures, obtaining maximum crystallinity at annealing temperatures of 160 °C. A plot of crystallinity versus the annealing temperatures indicates a linear relationship with the coefficient of determination (R^2 = 0.996) (see Supplementary Figure S1).

To confirm the degree of crystallinity of the PVOH coating films, the samples were tested using differential scanning calorimetry, where the enthalpy changes of the polymer crystals were determined during the heating cycles. Figure 2 shows the thermograms obtained for PVOH samples annealed at various temperatures. According to the results, the heating curves exhibited a broad endotherm at intervals of about 200 to 250 °C, which is

associated with the melting of the polymer studied. It can be observed that the endotherms shifted to higher temperature regions, which is reflected in the melting temperatures of the corresponding samples. An increase in melting temperatures can be seen with the PVOH samples prepared at different annealing temperatures. The minimum and maximum melting points of 203 and 225 °C were observed for PVOH-RT and PVOH-160 samples.

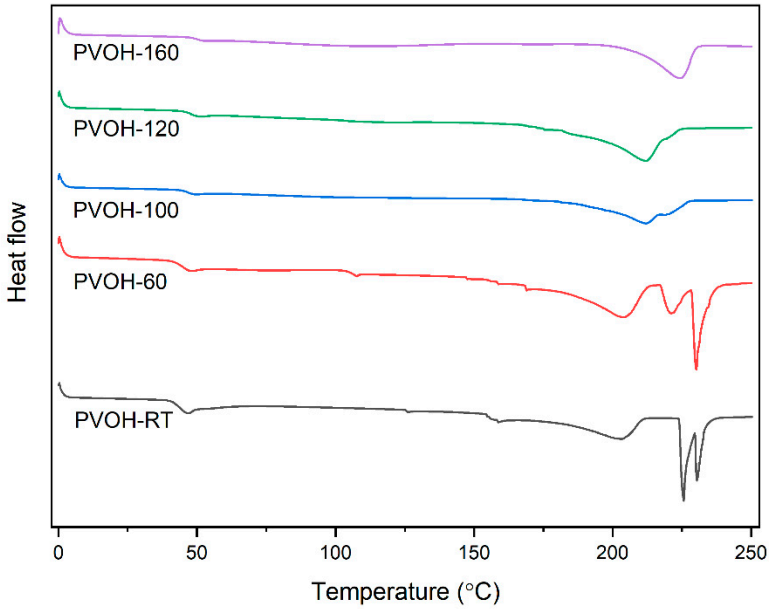

Figure 2. DSC thermograms for PVOH coating films prepared at different annealing temperatures.

The corresponding percentage of crystallinity was calculated according to Equation (2) and presented in Table 2. Although the calculated percentage crystallinity is lower than the FTIR-based calculations, the data follows the typical linearity trend for crystallinity versus the annealing temperature with the coefficient of determination (R^2 = 0.989) (see Supplementary Figure S2). Similar to FTIR data, the minimum of 31% and a maximum of 52% crystallinity were observed for PVOH-RT and PVOH-160, respectively. The increasing trend of crystallinity as a function of annealing temperatures is in good agreement with the work reported by Peppas [37].

Furthermore, the delaminated PVOH films were analyzed using the X-ray diffraction method; the degree of crystallinity of the samples was determined as the ratio of the area of crystalline peaks to the total area of peaks according to Equation (3). Figure 3 shows the X-ray diffraction pattern of PVOH samples. The positions of crystalline peak maxima in the diffraction pattern of higher crystalline were used as starting position. The starting position and half-width of the amorphous phase were 20° and 10°. Thus, the position for scattering maxima for crystalline phase, i.e., 11.2, 16.3 19.7, 22.8, and 26.2° are in good agreement with the reported literature [38].

According to the calculated peak areas corresponding to amorphous and crystalline peaks, the degree of crystallinity for PVOH samples was calculated and presented in Table 2. A maximum degree of crystallinity of 56% was obtained for PVOH-160. The results are similar to both the crystallinity fractions obtained from FTIR and DSC data. However, the linearity of the data points has substantially deviated with the coefficient of determination R^2 = 0.928 (see Supplementary Figure S3). More interestingly, the crystallinity versus annealing temperatures trend is complementary to the FTIR and DSC data findings. Therefore, with all the techniques used, the crystallinity of the PVOH films increased with the increase in annealing temperatures.

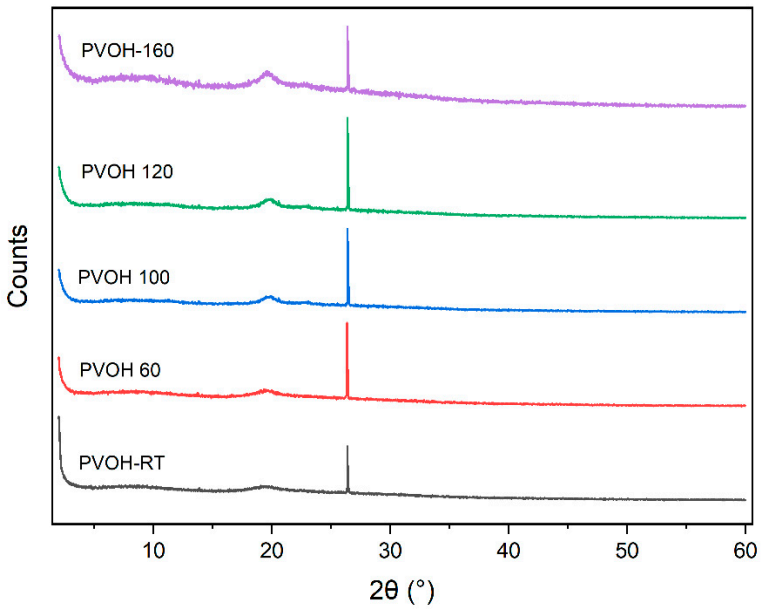

Figure 3. X-ray diffraction pattern for PVOH coating films prepared at different annealing temperatures.

Table 2. Sample names and crystallinity fraction of PVOH coating films.

S. No	Sample Names	Crystallinity		
		χ_c^{FTIR}	χ_c^{DSC}	χ_c^{XRD}
1	PVOH-RT	0.31	0.31	0.32
2	PVOH-60	0.37	0.35	0.34
3	PVOH-100	0.45	0.41	0.40
4	PVOH-120	0.47	0.45	0.45
5	PVOH-160	0.54	0.52	0.56

3.2. Barrier Performance

The oxygen transmission rate of the PVOH sample was measured in duplicates of each sample. The experimental OTR values, thickness measurements, and the calculation of O_2 permeability are presented in Table 3. Using the OTR values and thicknesses of samples, the O_2 permeability is calculated in (cc·µm/[m^2·h·atm]). In addition to the calculations, the thickness measurements of PVOH film is about 10 + 0.2 µm (see Table S1), which indicates the complete drying of the coating film. According to the results, the OTR or O_2 permeability values for PET substrate are significantly higher than those samples with PVOH coating film. Hence, the contribution of PET substrate to the barrier property is insignificant and thus conveniently neglected. A plot of O_2 permeability versus the crystallinity fractions obtained from the FTIR, DSC, and XRD data is shown in Figure 4. According to the results, it can be observed that an increase in the crystallinity of PVOH results in decreased oxygen permeability. For instance, based on FTIR data crystallinity values, for an increase in the degree of crystallinity from 0.31 to 0.47, the percentage decrease in oxygen permeability was observed to be 53.45%.

Table 3. Calculated oxygen permeability from OTR and thickness measurements, and respective confidence intervals (CI).

S. No.	Sample Names	OTR (cc/[m^2·day])		Thickness (μm)	Oxygen Permeability (cc·μm/[m^2·h·atm])			
		1	2		1	2	Average	CI
1	PET Sub.	15.90	15.78	118.0	78.15	77.58	77.87	-
2	PVOH-RT	1.88	1.58	128.2	10.03	8.44	9.24	5.00
3	PVOH-60	1.42	1.25	128.1	7.56	6.68	7.12	2.78
4	PVOH-100	1.08	1.18	127.8	5.75	6.25	6.00	1.58
5	PVOH-120	0.90	0.71	128.0	4.79	3.81	4.30	3.11
6	PVOH-160	0.21	0.47	127.9	1.12	2.51	1.81	4.41

Two combined factors can explain these observations; an increased crystallinity in the polymer either causes a prolonged diffusion time for oxygen (tortuous effects) and hence reduces the diffusivity or causes a reduced O_2 solubility in the crystalline regions, as reported by Grunlan et al. [18]. Considering the tortuous effects are more prominent, tortuosity-based models are appropriate for predicting barrier property in polymer systems with varying crystallinity.

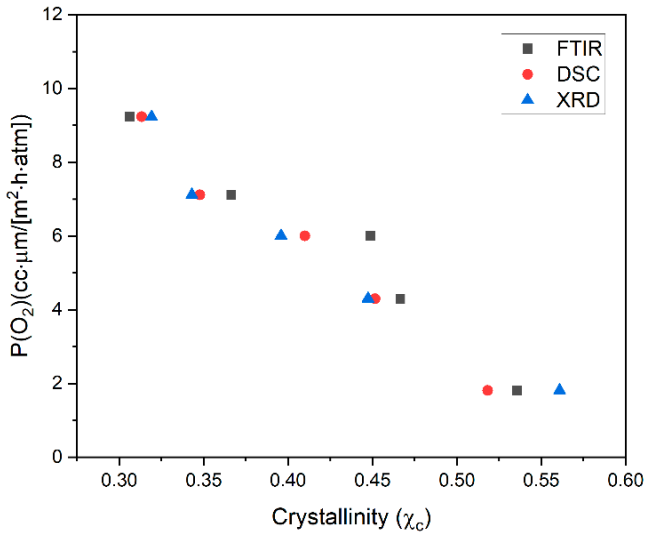

Figure 4. Oxygen permeability versus degree of crystallinity in PVOH coating films (Data points are with 90% confidence limit).

3.3. Model Predictions

Since PVOH is a semi-crystalline polymer, the fabrication of PVOH film without crystallinity is practically difficult. Therefore, the determination of oxygen permeability through the amorphous phase is carried out by extrapolating the experimentally obtained oxygen gas permeability data. The experimental relative permeabilities are thus calculated and compared with the modified Nielsen model-predicted relative permeability.

According to the comparison results shown in Figure 5, for orderly distributed crystallites, the modified Nielsen model (Equation (11)) predictions are in close agreement with the experimental data for equivalent lower aspect ratios of about 3.40. The average absolute error ranges from 4.61 to 5.79%, as shown in Table 4. However, with the case of randomly distributed crystallites, the modified Nielsen model Equation (12) was used to predict the relative permeability. According to the results, good agreements with experimental data were observed with AARE as low as 4.66%. However, these predictions are for a higher crystallite equivalent aspect ratio of about 10.40, as compared to the model prediction for orderly distributed crystallites.

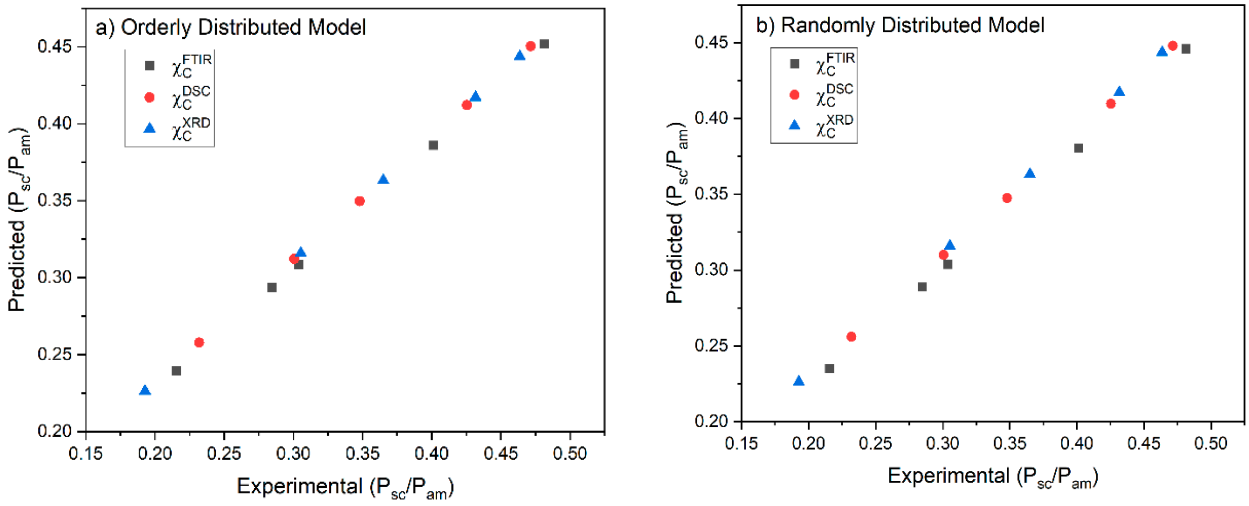

Figure 5. Comparison of experimental and predicted relative permeability using modified Nielsen model (**a**) for orderly distributed crystallites and (**b**) for randomly distributed crystallites.

Table 4. Crystallites aspect ratio and average absolute relative error of Nielsen model prediction orderly and randomly distributed crystallites.

S. No.	Crystallinity Data Source	Aspect Ratio (α = L/W)	AARE (%)	Crystallites Distribution
1	FTIR Data	3.502	5.18	Orderly
2	DSC Data	3.350	4.61	
3	XRD Data	3.350	5.79	
4	FTIR Data	10.90	4.66	Randomly
5	DSC Data	10.21	4.45	
6	XRD Data	10.05	5.79	

It seems that both the models, i.e., for orderly and randomly distributed, the predictions are within the acceptable range. It is obvious that considering the coating film preparation and the annealing temperature used to induce a varying degree of crystallinity in PVOH polymer, the crystallite, although platy-like lamellae, but the distribution of crystalline structures are expected to be uniform as the annealing time given is sufficiently enough to dry and induce crystallinities to a particular extent. Hence, in this case, the smaller aspect ratio of crystallite lamellae corresponding to the orderly distributed crystallites is more reliable than the randomly distributed crystallites with higher aspect ratios.

4. Conclusions

Poly (vinyl alcohol) coating films were prepared at different annealing temperatures to induce varying crystallinities. FTIR, DSC, and XRD techniques were used to characterize the resulting degree of crystallinities in the respective samples. Results indicate that with the increase in annealing temperature, the degree of crystallinity increased almost linearly. The oxygen barrier property of PVOH coating films was measured using an Ox-Tran oxygen transmission rate tester. The O_2 permeabilities were calculated from experimental OTR values. Results reveal that the barrier performance of PVOH coating film improved with the increase in the degree of crystallinity. This finding indicates that crystallites in PVOH film act as a barrier domain causing tortuous effects on the oxygen diffusion pathway. Hence, the tortuosity-based model can be conveniently employed to predict the barrier property of the semi-crystalline PVOH coating films. Modified Nielsen models for uniform and random distribution of crystalline regions were used to predict the relative permeability. The model predictions showed a good agreement with experimental results. For randomly distributed crystallites, the least average absolute relative errors

were observed for higher equivalent aspect ratios of about 10.4. For uniformly distributed crystallites, the predictions were also in good agreement but lower equivalent aspect ratios (around 3.4) of the crystallites.

Supplementary Materials: The following are available online at https://www.mdpi.com/article/10.3390/coatings11101253/s1, Figure S1: Linear fit of the degree of crystallinity of PVOH coating films determined using FTIR absorbance spectra versus annealing temperatures, Figure S2: Linear plot of the degree of crystallinity of PVOH films determined using DSC thermogram versus annealing temperatures, Figure S3: Linear fit of the degree of crystallinity of PVOH coating films determined using XRD diffractogram versus annealing temperatures, Table S1: Thickness measurement of PVOH coating film and PET substrate.

Author Contributions: Conceptualization, A.I. and B.M.; methodology, A.I.; validation, A.I.; formal analysis, M.L.; investigation, A.J., A.M. and M.L.; resources, B.M.; data curation, A.J.; writing—original draft preparation, A.I.; writing—review and editing, A.M.; supervision, A.M.; project administration, B.M. and M.L.; funding acquisition, B.M. All authors have read and agreed to the published version of the manuscript.

Funding: This research was funded by KK Foundation and Multi Barr industrial project (GA. No.: 20180036). The APC was funded by Karlstad University.

Institutional Review Board Statement: Not applicable.

Informed Consent Statement: Not applicable.

Data Availability Statement: Data is contained within the article and Supplementary Materials.

Acknowledgments: The authors of this work would like to appreciate the support given by the Department of Engineering and Chemical Sciences, Karlstad University, and the industry partners: Iggesund Paperboard AB, Cellcomb AB, OMYA, and UMV.

Conflicts of Interest: The authors declare no conflict of interest.

References

1. Ben Halima, N. Poly(vinyl alcohol): Review of its promising applications and insights into biodegradation. *RSC Adv.* **2016**, *6*, 39823–39832. [CrossRef]
2. Gaaz, T.S.; Sulong, A.B.; Akhtar, M.N.; Kadhum, A.A.; Mohamad, A.B.; Al-Amiery, A.A. Properties and Applications of Polyvinyl Alcohol, Halloysite Nanotubes and Their Nanocomposites. *Molecules* **2015**, *20*, 22833–22847. [CrossRef] [PubMed]
3. Pritchard, J.G. *Poly (Vinyl Alcohol): Basic Properties and Uses*; Macdonald: New York, NY, USA, 1970.
4. Musetti, A.; Paderni, K.; Fabbri, P.; Pulvirenti, A.; Al-Moghazy, M.; Fava, P. Poly(vinyl alcohol)-Based Film Potentially Suitable for Antimicrobial Packaging Applications. *J. Food Sci.* **2014**, *79*, E577–E582. [CrossRef] [PubMed]
5. Szabo, K.; Teleky, B.-E.; Mitrea, L.; Călinoiu, L.-F.; Martău, G.-A.; Simon, E.; Varvara, R.-A.; Vodnar, D.C. Active Packaging—Poly(Vinyl Alcohol) Films Enriched with Tomato By-Products Extract. *Coatings* **2020**, *10*, 141. [CrossRef]
6. Liu, Y.; Wang, S.; Lan, W.; Qin, W. Development of ultrasound treated polyvinyl alcohol/tea polyphenol composite films and their physicochemical properties. *Ultrason. Sonochem.* **2019**, *51*, 386–394. [CrossRef]
7. Wang, Y.; Li, J.; Guo, X.; Wang, H.; Qian, F.; Lv, Y. Active Biodegradable Polyvinyl Alcohol–Hemicellulose/Tea Polyphenol Films with Excellent Moisture Resistance Prepared via Ultrasound Assistance for Food Packaging. *Coatings* **2021**, *11*, 219. [CrossRef]
8. Toda, A. Small angle X-ray scattering from finite sequence of lamellar stacks of crystalline polymers. *Polymer* **2020**, *211*, 123110. [CrossRef]
9. Mallapragada, S.K.; Narasimhan, B. Infrared Spectroscopy in Analysis of Polymer Crystallinity. In *Encyclopedia of Analytical Chemistry*; Wiley & Sons: Hoboken, NJ, USA, 2006; pp. 1–14. [CrossRef]
10. Hagemann, H.; Snyder, R.G.; Peacock, A.J.; Mandelkern, L. Quantitative Infrared Methods for the Measurement of Crystallinity and its Temperature Dependence- Polyethylene. *Macromolecules* **1989**, *22*, 3600–3606. [CrossRef]
11. Desmaisons, J.; Rueff, M.; Bras, J.; Dufresne, A. Impregnation of paper with cellulose nanocrystal reinforced polyvinyl alcohol: Synergistic effect of infrared drying and CNC content on crystallinity. *Soft Matter* **2018**, *14*, 9425–9435. [CrossRef]
12. Kong, Y.; Hay, J.N. The measurement of the crystallinity of polymers by DSC. *Polymers* **2002**, *43*, 3873–3878. [CrossRef]
13. Shen, X.; Hu, W.; Russell, T.P. Measuring the Degree of Crystallinity in Semicrystalline Regioregular Poly(3-hexylthiophene). *Macromolecules* **2016**, *49*, 4501–4509. [CrossRef]
14. Hoffman, J.D.; Weeks, J.J. Specific Volume and Degree of Crystallinity of Semicrystalline Poly (chlorotrifluoroethylene), and Estimated Specific Volumes of the Pure Amorphous and Crystalline Phases. *J. Res. Natl. Bur. Stand.* **1958**, *6*, 465–479. [CrossRef]
15. Peterson, J.; TenCate, J.; Proffen, T.; Darling, T.; Nakotte, H.; Page, K. Quantifying amorphous and crystalline phase content with the atomic pair distribution function. *J. Appl. Crystallogr.* **2013**, *46*, 332–336. [CrossRef]

16. Tashiro, K.; Kitai, H.; Saharin, S.M.; Shimazu, A.; Itou, T. Quantitative Crystal Structure Analysis of Poly(vinyl Alcohol)–Iodine Complexes on the Basis of 2D X-ray Diffraction, Raman Spectra, and Computer Simulation Techniques. *Macromolecules* **2015**, *48*, 2138–2148. [CrossRef]
17. Tanaka, M.; Young, R.J. Molecular Orientation Distributions in the Crystalline and Amorphous Regions of Uniaxially Oriented Isotactic Polypropylene Films Determined by Polarized Raman Spectroscopy. *J. Macromol. Sci. Part B* **2007**, *44*, 967–991. [CrossRef]
18. Grunlan, J.C.; Grigorian, A.; Hamilton, C.B.; Mehrabi, A.R. Effect of clay concentration on the oxygen permeability and optical properties of a modified poly(vinyl alcohol). *J. Appl. Polym. Sci.* **2004**, *93*, 1102–1109. [CrossRef]
19. Vieth, W.R. *Diffusion in and through Polymers: Principles and Applications*; Hanser Publishers: New York, NY, USA, 1991.
20. Picard, E.; Espuche, E.; Fulchiron, R. Effect of an organo-modified montmorillonite on PLA crystallization and gas barrier properties. *Appl. Clay Sci.* **2011**, *53*, 58–65. [CrossRef]
21. Duan, Z.; Thomas, N.L. Water vapour permeability of poly(lactic acid): Crystallinity and the tortuous path model. *J. Appl. Phys.* **2014**, *115*, 064903. [CrossRef]
22. Tretinnikov, O.N.; Zagorskaya, S.A. Determination of the degree of crystallinity of poly(vinyl alcohol) by FTIR spectroscopy. *J. Appl. Spectrosc.* **2012**, *79*, 521–526. [CrossRef]
23. Nyflött, Å.; Moons, E.; Bonnerup, C.; Carlsson, G.; Järnström, L.; Lestelius, M. The influence of clay orientation and crystallinity on oxygen permeation in dispersion barrier coatings. *Appl. Clay Sci.* **2016**, *126*, 17–24. [CrossRef]
24. Carrera, M.C.; Erdmann, E.; Destéfanis, H.A. Barrier Properties and Structural Study of Nanocomposite of HDPE/Montmorillonite Modified with Polyvinylalcohol. *J. Chem.* **2013**, *2013*, 679567. [CrossRef]
25. Mallapragada, S.K.; Peppas, N.A. Dissolution mechanism of semicrystalline poly(vinyl alcohol) in water. *J. Polym. Sci. Part B Polym. Phys.* **1996**, *34*, 1339–1346. [CrossRef]
26. Peppas, N.A.; Merrill, E.W. Differential scanning calorimetry of crystillized PVA hydrogels. *J. Appl. Polym. Sci.* **1976**, *20*, 1457–1465. [CrossRef]
27. Gaidukov, S.; Danilenko, I.; Gaidukova, G. Characterization of Strong and Crystalline Polyvinyl Alcohol/Montmorillonite Films Prepared by Layer-by-Layer Deposition Method. *Int. J. Polym. Sci.* **2015**, *2015*, 123469. [CrossRef]
28. Aziz, S.B.; Marf, A.S.; Dannoun, E.M.A.; Brza, M.A.; Abdullah, R.M. The Study of the Degree of Crystallinity, Electrical Equivalent Circuit, and Dielectric Properties of Polyvinyl Alcohol (PVA)-Based Biopolymer Electrolytes. *Polymers* **2020**, *12*, 2184. [CrossRef]
29. International, A. Standard Test Method for Oxygen Gas Transmission Rate through Plastic Film and Sheeting Using a Coulometric Sensor. In *ASTM D3985-05*; ASTM: West Conshohocken, PA, USA, 2005.
30. Introzzi, L.; Blomfeldt, T.O.; Trabattoni, S.; Tavazzi, S.; Santo, N.; Schiraldi, A.; Piergiovanni, L.; Farris, S. Ultrasound-assisted pullulan/montmorillonite bionanocomposite coating with high oxygen barrier properties. *Langmuir* **2012**, *28*, 11206–11214. [CrossRef]
31. Lin, H.; Freeman, B.D. Gas solubility, diffusivity and permeability in poly(ethylene oxide). *J. Membr. Sci.* **2004**, *239*, 105–117. [CrossRef]
32. Nielsen, L.E. Models for the Permeability of Filled Polymer Systems. *J. Macromol. Sci. Part A Chem.* **1967**, *1*, 929–942. [CrossRef]
33. Zid, S.; Zinet, M.; Espuche, E. Modeling diffusion mass transport in multiphase polymer systems for gas barrier applications: A review. *J. Polym. Sci. Part B Polym. Phys.* **2018**, *56*, 621–639. [CrossRef]
34. Abdullah, Z.W.; Dong, Y.; Han, N.; Liu, S. Water and gas barrier properties of polyvinyl alcohol (PVA)/starch (ST)/glycerol (GL)/halloysite nanotube (HNT) bionanocomposite films: Experimental characterisation and modelling approach. *Compos. Part B Eng.* **2019**, *174*, 107033. [CrossRef]
35. Idris, A.; Man, Z.; Maulud, A.S.; Uddin, F. Modified Bruggeman models for prediction of CO_2 permeance in polycarbonate/silica nanocomposite membranes. *Can. J. Chem. Eng.* **2017**, *95*, 2398–2409. [CrossRef]
36. Kenney, J.F.; Willcockson, G.W. Structure-Property relationships of poly(vinyl alcohol). III. Relationships between stereo-regularity, crystallinity, and water resistance in poly(vinyl alcohol). *J. Appl. Polym. Sci. A-1 Polym. Chem.* **1966**, *4*, 679–698. [CrossRef]
37. Peppas, N.A. Infrared Spectroscopy of Semicrystalline Poly(vinyl alcohol) Networks. *Makromol. Chem* **1977**, *178*, 595–601. [CrossRef]
38. Minus, M.L.; Chae, H.G.; Kumar, S. Single wall carbon nanotube templated oriented crystallization of poly(vinyl alcohol). *Polymer* **2006**, *47*, 3705–3710. [CrossRef]